Journal of Chemical Health Risks

www.jchr.org

JCHR (2024) 14(4), 271-288 | ISSN:2251-6727

Discovery of COVID-19 Inhibitors from Medicinal Plants via Molecular Docking and Molecular Dynamics Study

Brajendra Singh*, Shailesh Pathak, Dr Pawan Tiwari, Dr Manoj Kumar Mishra, Shashi Singh
Shambhunath Institute of Pharmacy, Jhalwa, Prayagraj, U. P, India.

(Received: 14 April 2024 Revised: 1 May 2024 Accepted: 18 June 2024)

KEYWORDS
Carissa edulis, Geranium Sanguin Eu, Guazuma Ulmifolia, Polygonum cuspidatum, Saxifraga melanocentra, Molecular Docking, Molecular Dynamics,

ABSTRACT:
Through in-silico screening, compounds from Carissa edulis, Geranium sanguineum, Guazuma ulmifolia, Polygonum cuspidatum, and Saxifraga melanocentra were identified as potential inhibitors of COVID-19. The results indicated that quercetin-3-O-β-d-glucopyranoside, kaempferol-3-O-β-d-glucopyranoside, isorhamnetin-3-O-β-d-glucopyranoside, and (+)-butyl-O-α-l-rhamnoside have high potential against the main protease, 3CLpro, of SARS-CoV-2

Introduction

The global pandemic of coronavirus disease 2019 (COVID-19), caused by severe acute respiratory syndrome coronavirus 2 (SARS-CoV-2), has resulted in a critical and immediate public health crisis. SARS-CoV-2 is a novel variant of the coronavirus that emerged in China in December 2019 [1-4]. The symptoms of COVID-19 might be vague and those who are infected may not display any symptoms. Individuals who contract COVID-19 typically have various symptoms such as moderate respiratory issues, fever, dry cough, exhaustion, difficulty breathing, and loss of smell. These symptoms usually manifest about 5-6 days after infection, however the timeframe can vary from two to fourteen days. Possible complications encompass pneumonia and acute respiratory distress syndrome, both of which can result in mortality [5-7].

Thus far, there has been no discernible advancement in the management of this disease, and the patient is still receiving treatment based on their observable symptoms that have been diagnosed. Currently, there is no established vaccination or targeted antiviral therapy available. The Human Genome Project facilitated the identification of a greater number of novel therapeutic targets for the purpose of drug discovery. [8-10] Concurrently, advanced methods for purifying proteins, such as high-throughput techniques, as well as crystallography and nuclear magnetic resonance spectroscopy techniques, have played a significant role in revealing the precise structural characteristics of proteins and protein complexes.These advancements enable computational tactics to permeate several fields, including the utilization of virtual screening approaches (VSto ascertain outcomes and enhance molecular methodologies. Molecular docking is a computer method that is employed to assess the strength of interaction between two molecules, such as ligand-protein and protein-protein. Molecular docking has become a crucial element in the process of drug discovery. These approaches are also useful for anticipating the adverse and hazardous effects of substances. Several standard medications, including chloroquine, hydroxychloroquine, and remediffer, have undergone laboratory testing and demonstrated a distinct therapeutic effect. Nevertheless, the clinical pharmacological response is discouraging and toxicity continues to be an unavoidable issue that leads to severe side effects. Due

Journal of Chemical Health Risks
www.jchr.org
JCHR (2024) 14(4), 271-288 | ISSN:2251-6727

to the absence of a targeted treatment for COVID-19, researchers worldwide have turned to medicinal plants recognized in the field of ethnopharmacology for their antiviral properties. [11-14] The emergence of viral resistance to existing antiviral drugs underscores the necessity for novel and potent chemicals to combat viral infections. This study focuses on identifying active compounds found in medicinal plants used in Sudanese traditional medicine for treating viral diseases. The compounds were selected based on a literature review and were subjected to docking studies to understand their interactions. The aim was to determine which molecules are most effective in inhibiting the SARS-CoV-2 main protease enzyme, with the goal of finding potential treatments for COVID-19. The results were then compared to the effects of proposed drugs like chloroquine and hydroxychloroquine. Additionally, the toxicity of these compounds was evaluated to determine their suitability for human consumption. Understanding the crystal structure of therapeutic targets is essential for predicting the future discovery of medications. While certain viral illnesses can be effectively treated with licensed antiviral medications, there are currently no vaccinations or treatments available for others. The majority of the authorized antiviral medications are either directly or indirectly associated with adverse effects. hence necessitating the development of antiviral drugs based on natural phytochemicals. Internationally, there is a trend towards using plant-derived medications for antiviral purposes due to their lower toxicity and less likelihood of acquiring resistance. A diverse range of chemicals from various groups were chosen based on their chemical origin and utilized for the treatment of numerous ailments, including antiviral activity. [15-17] The objective of this study is to discover the active components of natural plants, considering the current circumstances and the various medicinal uses of plants such as *Carissa edulis*, *Geranium Sanguin Eu*, *Guazuma Ulmifolia*, *Polygonum cuspidatum*, *Saxifraga melanocentra* as probable drug leads against COVID-19. The objective of this research endeavor was to discover innovative inhibitors targeting SARS COVID-19.

Experimental Work

Preparation of Protein

The system must be carefully selected and prepared before doing any calculations. The first step is to obtain a structure of the protein, preferably with a bound ligand. It is highly recommended to consider three-dimensional structures with high resolution or structures co-crystallized with high affinity ligands or natural substrates.[18] Molecular optimization was carried out for main protease of 6LU7 as a preparative process for docking. The Structure of COVID-19 main protease in complex with an inhibitor N3 (PDB ID: 6LU7) was downloaded from the RCSB PDB (Protein Data Bank) database. [20-21] The protein structure integrity was checked and adjusted, and missing residues near the active site were added using Autodock Tool.[22] The Graphical User Interface program ‘‘Autodock Tools’’ was used to prepare, run, and analyze the docking simulations. Kollman united atom charges, solvation parameters and polar hydrogens were added to the receptor for the preparation of protein in docking simulation. Since ligands are not peptides, Gasteiger charge was assigned and then non-polar hydrogens were merged. Autodock requires pre-calculated grid maps, one for each atom type, present in the ligand being docked as it stores the potential energy arising. [23-24] This grid must surround the region of interest (active site) in the macromolecule. The protein−ligand complex was subjected to geometry refinement using an uff forcefield. [25]

Ligand preparation

A set of 77 compounds selected to perform the molecular docking studies to screen and identify the potent antiviral agents specifically for COVID-19.[26] The structures of the following active compounds of ***Carissa edulis (Babool), Geranium Sanguin Eu, Guazuma Ulmifolia, Polygonum cuspidatum, Saxifraga melanocentra*** were drawn using ChemDraw software and energy minimization by uff (universal force field) using open Babel.

Compound screening using PyRx

Molecular testing of all the compound libraries was performed using the PyRx software by Autodock wizard as the engine for docking. During the docking period, the ligands were considered to be flexible, and the protein was supposed to be rigid. The configuration file for the grid parameters was generated using Grid box for 6LU7 (x = -11.08, y = 12.67, z = -69.44) in PyRx respectively and also performed the docking of Human Proteases compounds.[27-28] The energy minimization of the all

Journal of Chemical Health Risks

www.jchr.org

JCHR (2024) 14(4), 271-288 | ISSN:2251-6727

compounds was done by employing open. Molecular docking was done using Autodock Vina.

The configuration file for the grid parameters was generated using Grid box (size 25, 25, 25) for 6LU7 (x = -11.0819258203, y = 12.6709418567, z = 69.4407720834) in PyRx respectively. The application was also used to know/predict the amino acids in the active site of the protein that interact with the ligands. The results less than 2.0 Å in positional root-mean-square deviation (RMSD) was considered ideal and clustered together for finding the favorable binding. The highest binding energy (most negative) was recognized as the ligand with maximum binding affinity. [29]

Analysis and visualization

Visual examination of the docking site was performed using Biovia Drug discovery studio 2019, ligplot and the results were validated using the ADT tool. [30]

Molecular docking process

The docking was done using Autodock in PyRx. After the run, the out files stored in the user folder where the path run was specified in the edit preference. These output files were stored in PDBQT files, each having fifty poses. The Autodock application file was launched which then showed the empty dashboard along with "File" on the left-hand corner of the page. The Out-file models were loaded using the "read molecule" application from the selected-out file folder. Different poses were analyzed in the Autodock tool.

The grid box was determined as center the coordinates X: -20.5916, Y: 18.6168, and Z: -26.0872, while as dimension the coordinates X: 28.5863, Y: 22.8561, and Z: 24.5182. The pose with the lowest binding energy in kcal/mol was selected for further analysis. The docked molecules were then further converted into PDB format in PyMol and their interaction was studied using the software LigPlot+ v.1.4.5. The All-compound poses were first docked against the virus main protease to check their binding energy. The interaction of all these compounds with the COVID-19 main protease could later be utilized for getting the hits. [31-32]

Ligand Based Drug likeness, ADME/Toxicity properties

Many potential therapeutic agents fail to reach the clinic trials because of their unfavorable absorption, distribution, metabolism, and elimination (ADME) parameters; also, it is not checking the drug likeness. Lipinski's rule of five Veber's rule, Egan's rule, Veber's rule, Egan's rule and polar surface area (TPSA) and number of rotatable bonds were calculated using SwissADME tool, Molinspiration and PkCSM. [33-34]

Molecular Dynamics (MD) Simulations

The structural and dynamic transition at the atomistic level in the COVID-19 main protease (6LU7) upon binding of small molecules (top 4) were investigated by using MD simulations. [35] Molecular dynamics simulation was carried out using Desmond 2021-4 on an Acer workstation installed with Ubuntu 22.04. For the Complex, the force field was processed with an OPLS-2005 Force field, for generating the topology. The complex was prepared using the system builder platform by solvation with the simple point-charge (SPC) explicit water model in the orthorhombic simulation box. The solvated complex system was neutralized with a suitable number of Na + /Cl − counter ions and a salt concentration of 0.15 M to mimic the physiological conditions. The receptor–ligand complex system was designated with the OPLS-2005 force field, and an explicit solvent model with the SPC water molecules was used in this system in an orthorhombic box. Desmond Minimization of systems was performed for 100 ps and the systems were relaxed using BioLuminate default protocol then the simulations were carried out at 300 K temperature and 1.0325 bar pressure for 100ns.[36]

Results and Discussion

We have a set of docked 77 components of *Carissa edulis*, *Geranium Sanguin Eu*, *Guazuma Ulmifolia*, *Polygonum cuspidatum*, *Saxifraga melanocentra* the binding affinity, H-Bond interaction, and Interactive amino acids of natural compounds toward spike protein and in the top 4 Human protease agents docking result based on bonding energy and H-Bond interaction and Interactive amino acids.

Journal of Chemical Health Risks
www.jchr.org
JCHR (2024) 14(4), 271-288 | ISSN:2251-6727

Table 1: Docking interactions and binding affinity of top 4 compounds with 6lu7 *Carissa edulis*

Compound name	**Hydrophobic Interactions**	H bond	Binding Affinity
quercetin-3-O-β-d glucopyranoside	**CYS44,TYR54,PRO52,MET49,LEU27,PHE140,LEU141,CYS145,MET165**	**SER144**	**-9.2**
	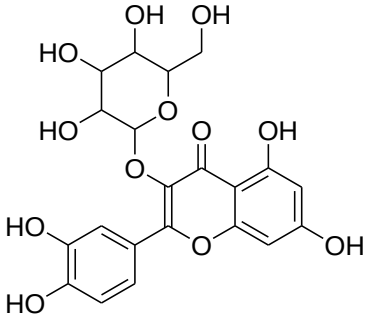		
kaempferol-3-O-β-d-glucopyranoside	**CYS44,TYR54,MET49,140,LEU141,MET165,CYS145,**	**-**	**-9**
	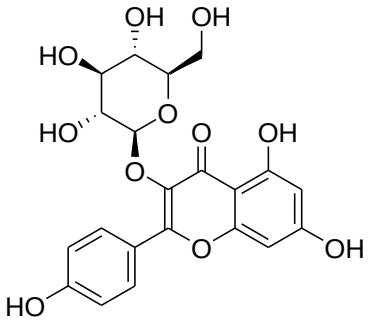		
isorhamnetin-3-O-β-d-glucopyranoside	**CYS44,TYR54,PRO52,MET49,CYS145,LEU141,PHE140,MET165**	**GLU166**	**-8.9**
	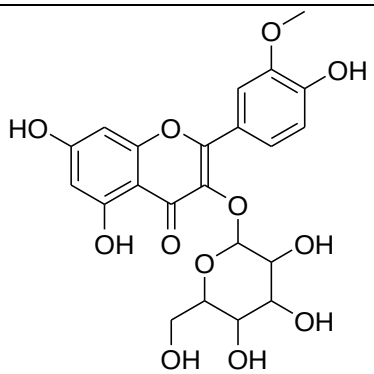		
(+) butyl-O-α-l-rhamnoside	**TYR54,PRO52,CYS44,MET49,CYS145,MET165,LEU141,PHE140**		**-8.6**

Journal of Chemical Health Risks
www.jchr.org
JCHR (2024) 14(4), 271-288 | ISSN:2251-6727

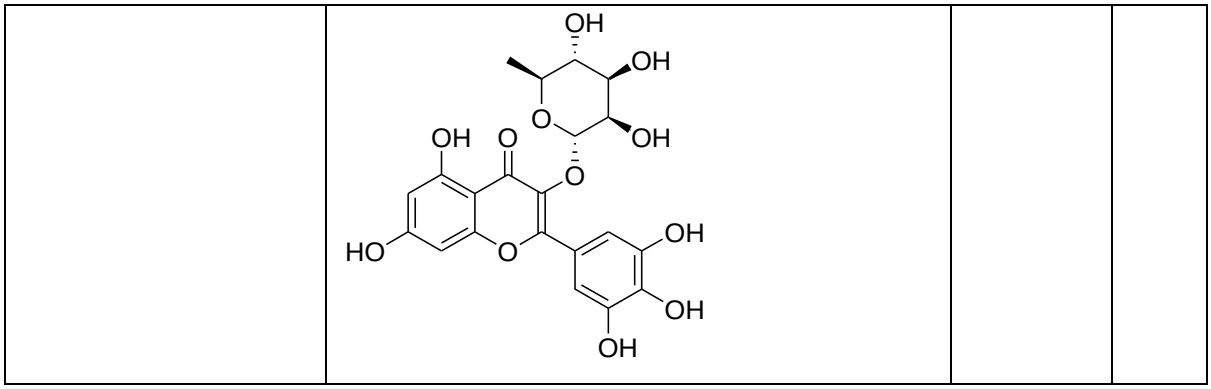

Table 1 shows the results obtained from the molecular docking carried out on all the molecules present in *Carissa edulis*, *Geranium Sanguin Eu*, *Guazuma Ulmifolia*, *Polygonum cuspidatum*, *Saxifraga melanocentra* or reference molecule, and Table 1 shows the results of top 4 molecules from human protease library (quercetin-3-O-β-d glucopyranoside with **-9.2** docking score, kaempferol-3-O-β-d-glucopyranoside with **-9** docking score, isorhamnetin-3-O-β-d-glucopyranoside with **-8.9** docking score, (+) butyl-O-α-l-rhamnoside with **-8.6** docking score), by giving the interaction energy for each compound, there is a difference in energy between each ligand and COVID-19 spike protein.

Comparison shows, quercetin-3-O-β-d glucopyranoside, kaempferol-3-O-β-d-glucopyranoside, isorhamnetin-3-O-β-d-glucopyranoside and (+) butyl-O-α-l-rhamnoside have the higher binding affinity and batter interaction with protein in comparison of other compounds. The quercetin-3-O-β-d glucopyranoside has binding affinity (-9.2 kcal/mol), Hydrophobic Interactions are CYS44, TYR54, PRO52, MET49, LEU27, PHE140, LEU141, CYS145, MET165, and SER144 and Thr26 shown H-bond interaction with protein in **fig. 1**.

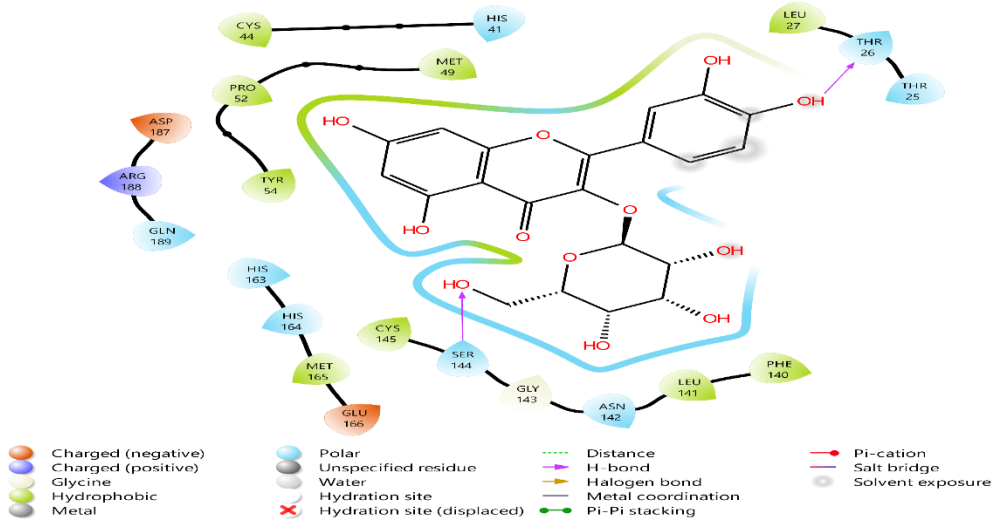

Fig. 1: 2D interactions for 6lu7_quercetin-3-O-β-d glucopyranoside

The kaempferol-3-O-β-d-glucopyranoside has a binding affinity (-9 kcal/mol), CYS44, TYR54, MET49, 140, LEU141, MET165, and CYS145 showed Hydrophobic Interactions with protein in **fig. 2**.

Journal of Chemical Health Risks
www.jchr.org
JCHR (2024) 14(4), 271-288 | ISSN:2251-6727

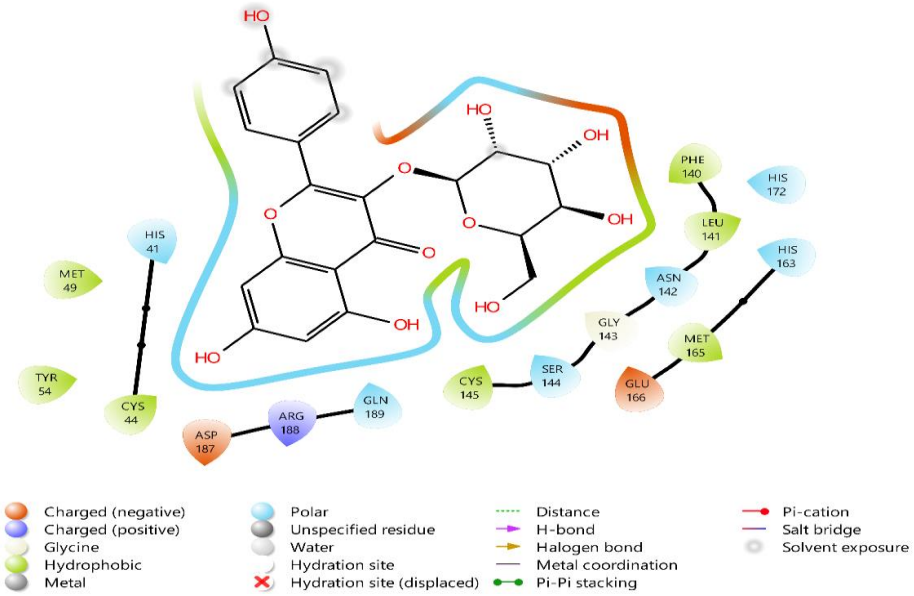

Fig. 2: 2D interactions for 6lu7_kaempferol-3-O-β-d-glucopyranoside

The isorhamnetin-3-O-β-d-glucopyranoside has a binding affinity (-8.9 kcal/mol), Hydrophobic Interactions are CYS44, TYR54, PRO52, MET49, CYS145, LEU141, PHE140, and MET165, and GLU166 showed H-bond interactions with protein in **fig. 3**.

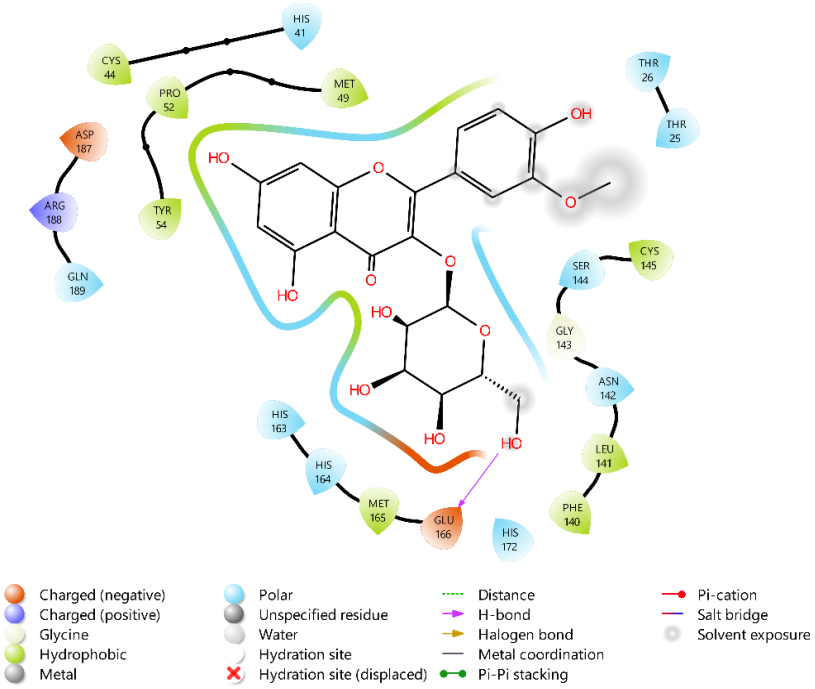

Fig. 3: 2D interactions for 6lu7_isorhamnetin-3-O-β-d-glucopyranoside

The (+) butyl-O-α-l-rhamnoside has a binding affinity (-8.6 kcal/mol) and Hydrophobic Interactions are TYR54, PRO52, CYS44, MET49, CYS145, MET165, LEU141, and PHE140 with 6LU7 in **fig. 4**.

Journal of Chemical Health Risks
www.jchr.org
JCHR (2024) 14(4), 271-288 | ISSN:2251-6727

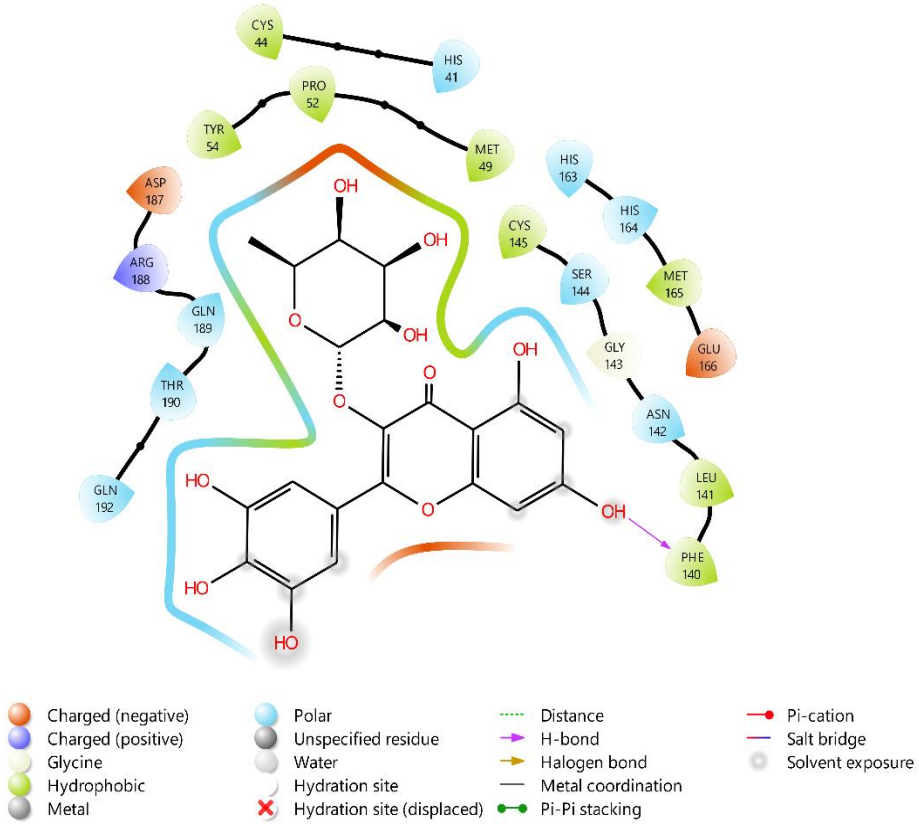

Fig. 4: 2D interactions for 6lu7_(+) butyl-O-α-l-rhamnoside

ADME Studies

Compound	Molecular weight	Num. rotatable bonds	Num. H-bond acceptors	Num. H-bond donors	TPSA (Å²)	Log Po/w (iLOGP)	GI absorption	Lipinski	Predicted % Absorption
quercetin-3-O-β-d glucopyranoside	464.38 g/mol	4	12	8	210.51 Å²	2.11	Low	No; 2 violations: NorO>10, NHorOH>5	
kaempferol-3-O-β-d-glucopyranoside	448.38 g/mol	4	11	7	190.28 Å²	1.29	Low	No; 2 violations: NorO>10, NHorOH>5	

Journal of Chemical Health Risks
www.jchr.org
JCHR (2024) 14(4), 271-288 | ISSN:2251-6727

isorhamnetin-3-O-β-d-glucopyranoside	478.40 g/mol	5	12	7	199.51 Å²	1.21	Low	No; 2 violations: NorO>10, NHorOH>5	
(+) butyl-O-α-l-rhamnoside	464.38 g/mol	3	12	8	210.51 Å²	1.71	Low	No; 2 violations: NorO>10, NHorOH>5	

ADME studies performed using Swiss ADME tool and all the compounds here follow lipinski's Rule of Five.

Molecular Dynamics Results

Molecular dynamics simulation was carried out using Desmond 2021-4 on an Acer workstation installed with Ubuntu 22.04. For the **quercetin-3-O-β-d glucopyranoside-6LU7** Complex, the force field was processed with an OPLS-2005 Force field, for generating the topology (VanDerSpoelet al. 2005). The receptor-ligand complex system was designated with the OPLS-2005 force field, and an explicit solvent model with the SPC water molecules was used in this system in an orthorhombic box. Desmond Minimization of systems was performed for 100 ps and the systems were relaxed using BioLuminate default protocol then the simulations were carried out at 300 K temperature and 1.0325 bar pressure for 100ns.

Complex 1: 6LU7-quercetin-3-O-β-d glucopyranoside

MD simulation at 100ns was performed for top-docked compound **quercetin-3-O-β-d glucopyranoside**. MD simulations were carried out to determine the stability of the interactions of ligand-protein docked complexes. In MD simulations, the stability of the protein (6LU7) with mechanism-based inhibitor (N3) bound at the Targeting main protease (M^{pro}) of SARS-CoV-2: M^{pro} binding site was investigated using RMSD analysis of the protein backbone about the initial frame structure. The RMSD value of protein was stable between 2.0 to 2.8 Å from a 20 to 100 ns time frame. The ligand RMSD was stable between 1.8 to 2.8 Å from a 50 to 100 ns time frame and showed some fluctuation between 10 to 50 ns (Figure 5). The RMSF plots of protein (side chains) and ligand showed few fluctuations between 0.7 to 2.5 Å respectively, and Protein residues that interact with the ligand are marked with green-colored vertical bars (Figure 6) The interactions during the 100 ns trajectory were examined, where residues Asp187, Thr26, and Gln189 showed H-Bond interaction with protein, and His41 were involved in π-π stacking interactions with protein, Cys22, Thr24, Thr25, Arg40, Thr45, Tyr54, val186, and Gln189 were engaged in hydrophobic interactions with protein (Figure 7, 8).

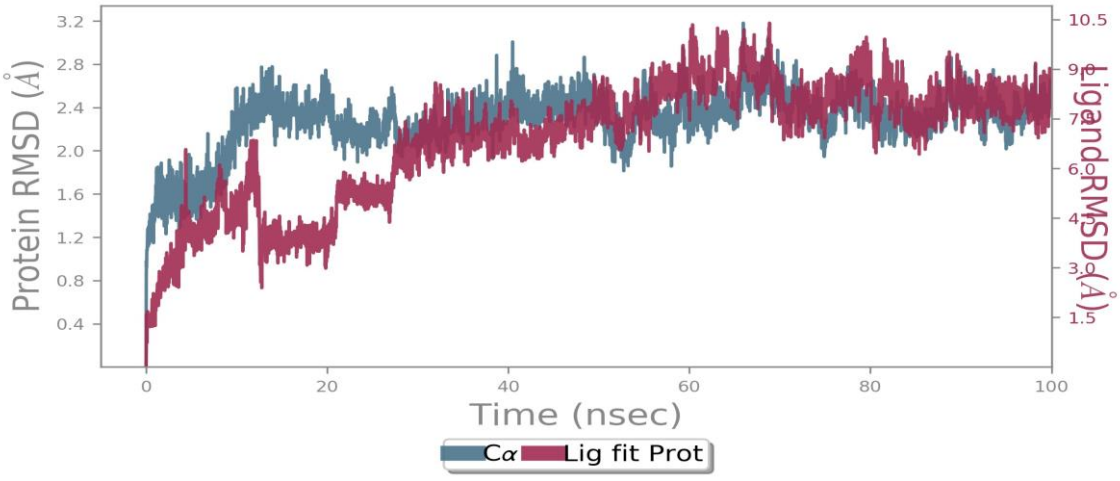

Fig.5: RMSD plot of coronavirus for COVID-19 (6LU7) with and without **quercetin-3-O-β-d glucopyranoside** as a function of time

Journal of Chemical Health Risks
www.jchr.org
JCHR (2024) 14(4), 271-288 | ISSN:2251-6727

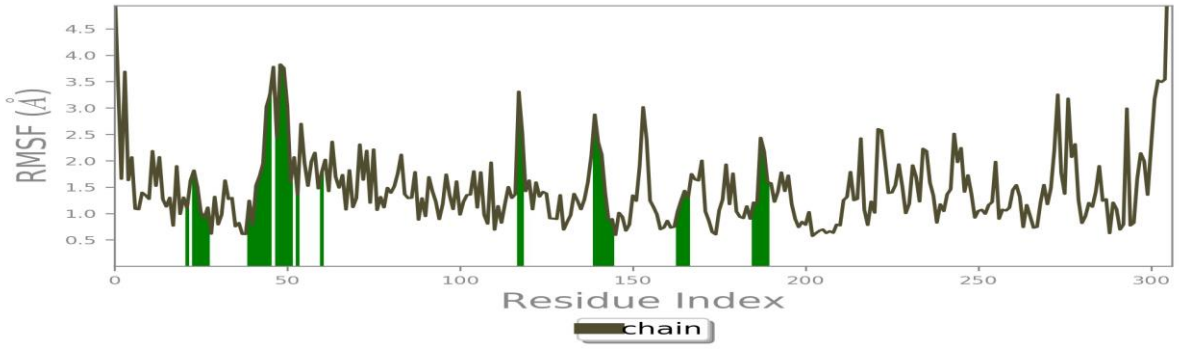

Fig.6: RMSF plot of coronavirus for COVID-19 (6LU7) with and without **quercetin-3-O-β-d glucopyranoside** at 100 ns time scale

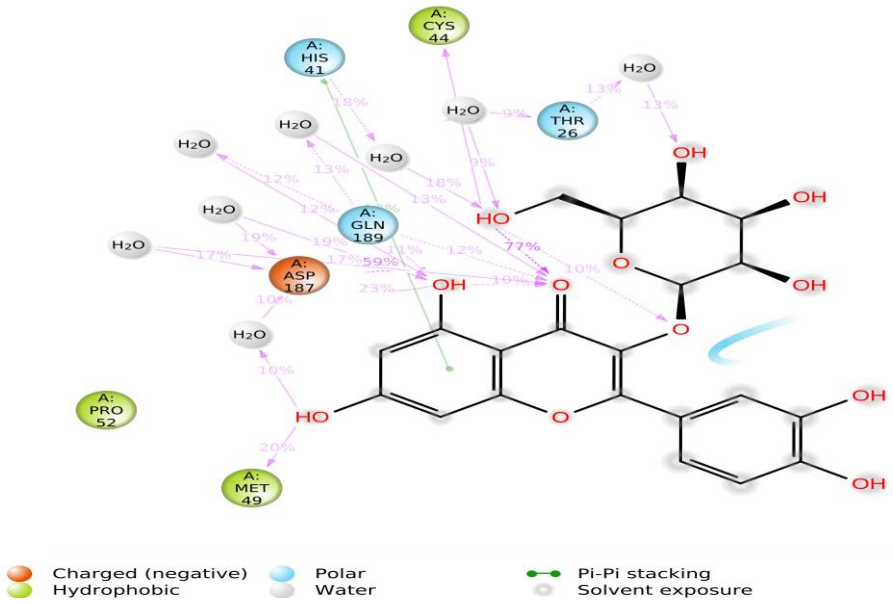

Fig.7: The interaction of top hit molecule **quercetin-3-O-β-d glucopyranoside** with coronavirus for COVID-19 (6LU7)

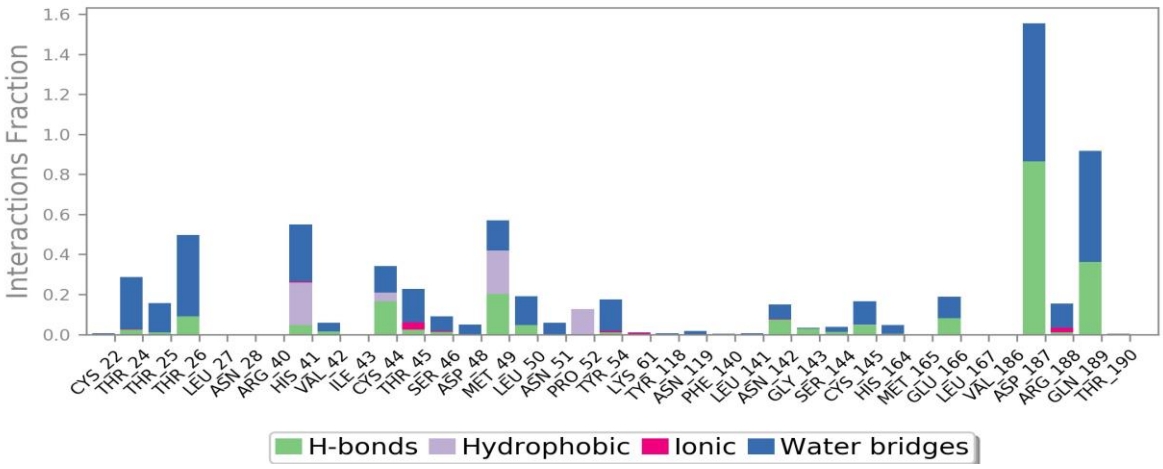

Fig.8: Protein-ligand contacts for compound **quercetin-3-O-β-d glucopyranoside**

Journal of Chemical Health Risks
www.jchr.org
JCHR (2024) 14(4), 271-288 | ISSN:2251-6727

Complex 2: 6LU7-kaempferol-3-O-β-d-glucopyranoside

MD simulation at 100ns was performed for top-docked compound **kaempferol-3-O-β-d-glucopyranoside**. MD simulations were carried out to determine the stability of the interactions of ligand-protein docked complexes. In MD simulations, the stability of the protein (6LU7) with mechanism-based inhibitor (N3) bound at the Targeting main protease (M^{pro}) of SARS-CoV-2: M^{pro} binding site was investigated using RMSD analysis of the protein backbone about the initial frame structure. The RMSD value of protein was stable between 1.3 to 2.0 Å from a 10 to 100 ns time frame it showed excellent stability with protein. The ligand RMSD was also stable between 5.3 to 6.7 Å from a 10 to 100 ns time frame and showed some fluctuation before 10 ns (Figure 9). The RMSF plots of protein (side chains) and ligand showed few fluctuations between 0.8 to 2.5 Å respectively, and Protein residues that interact with the ligand are marked with green-colored vertical bars (Figure 10) The interactions during the 100 ns trajectory were examined, where residues Asn142, Glu166, Asp187, Arg188, and Gln189 showed H-Bond interaction with protein, and His41, Met49, and Met165 were engaged in hydrophobic interactions with protein and polar interactions with His41 and Gln189 (Figure 11, 12).

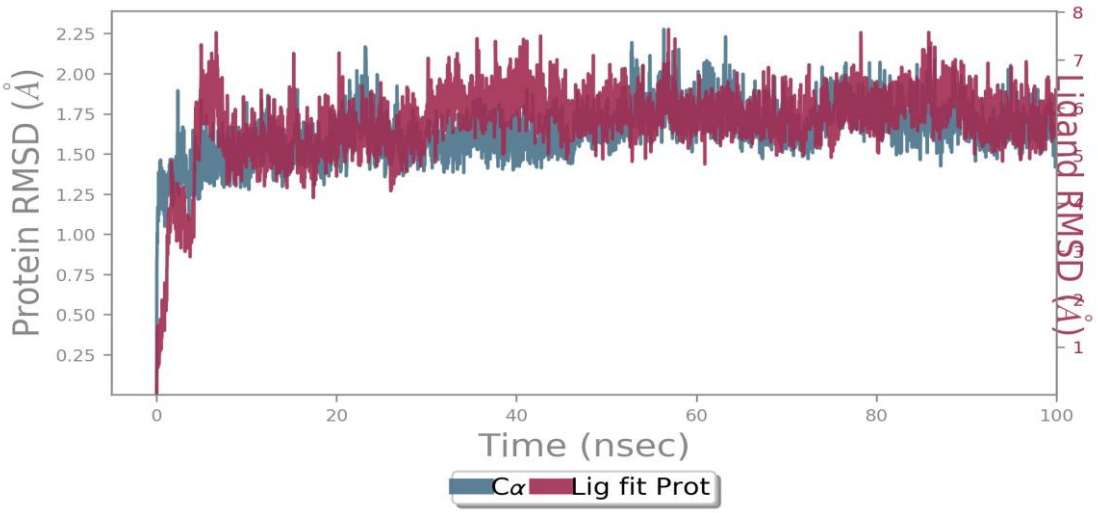

Fig.9: RMSD plot of coronavirus for COVID-19 (6LU7) with and without **kaempferol-3-O-β-d-glucopyranoside** as a function of time

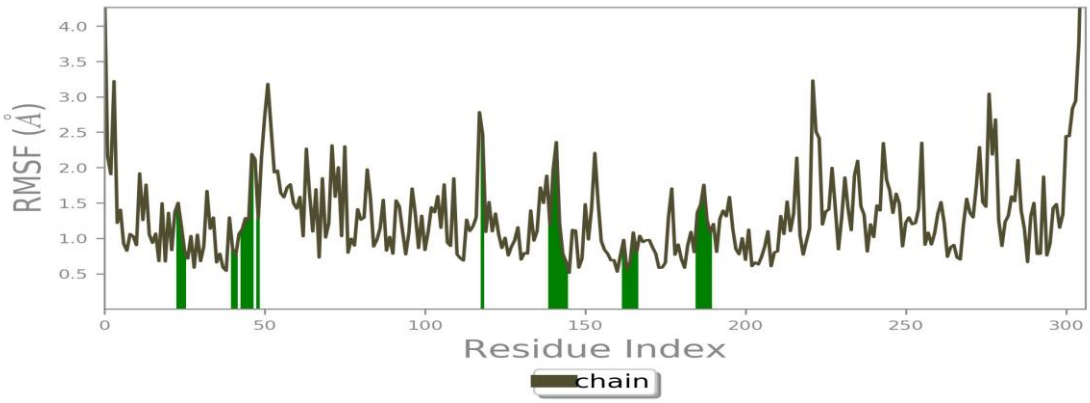

Fig.10: RMSF plot of coronavirus for COVID-19 (6LU7) with and without **kaempferol-3-O-β-d-glucopyranoside** at 100 ns time scale

Journal of Chemical Health Risks
www.jchr.org
JCHR (2024) 14(4), 271-288 | ISSN:2251-6727

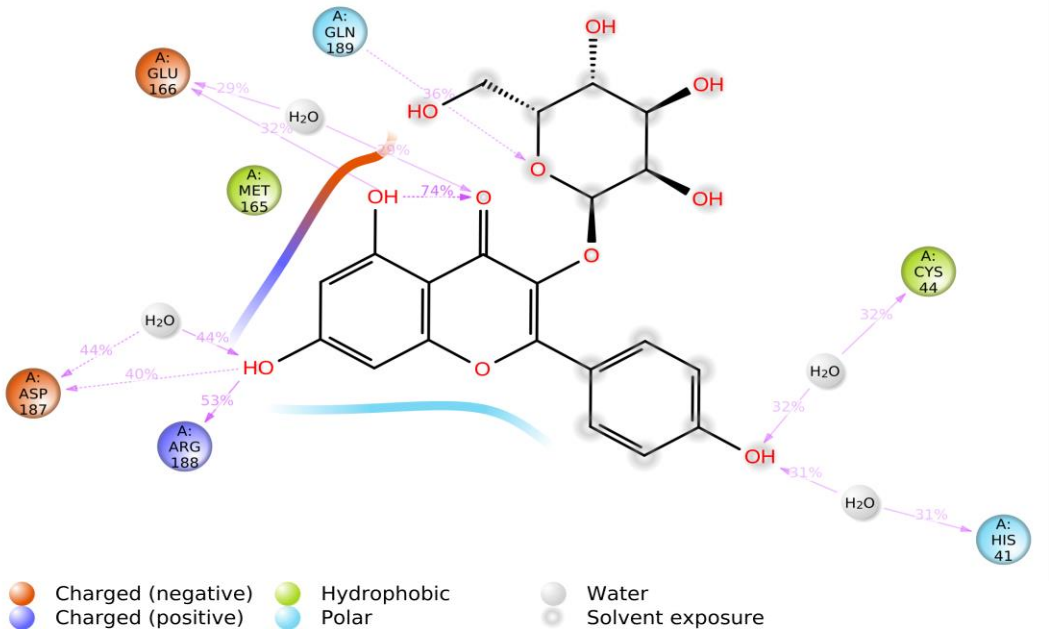

Fig.11: The interaction of top hit molecule **kaempferol-3-O-β-d-glucopyranoside** with coronavirus for COVID-19 (6LU7)

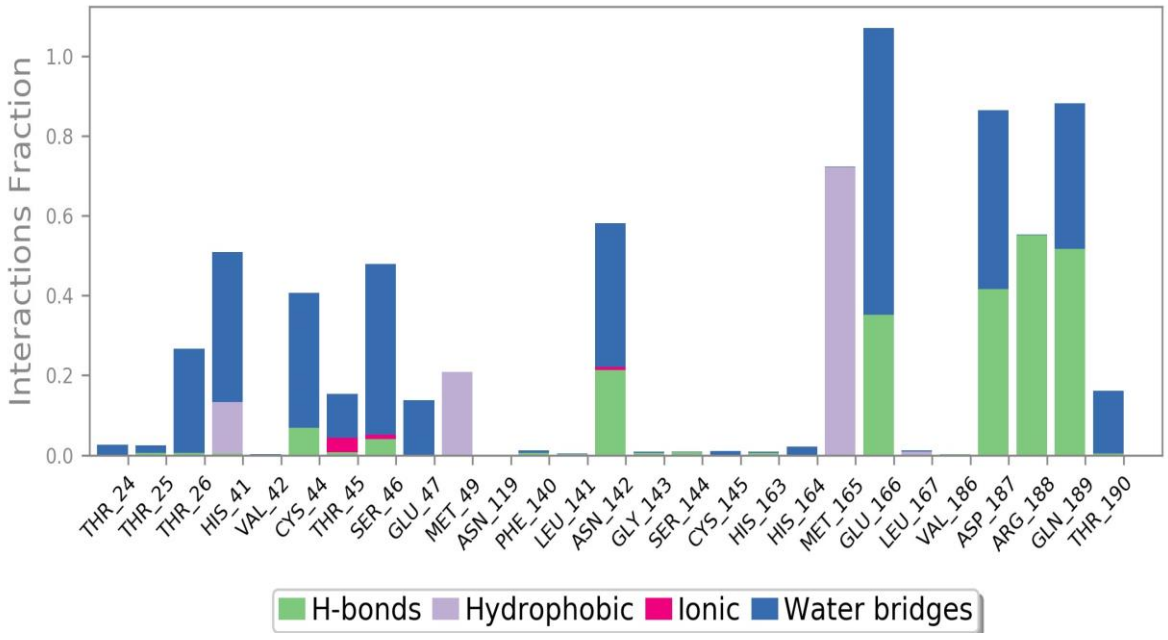

Fig.12: Protein-ligand contacts for compound **kaempferol-3-O-β-d-glucopyranoside**

Complex 3: 6LU7-isorhamnetin-3-O-β-d-glucopyranoside

MD simulation at 100ns was performed for top-docked compound **isorhamnetin-3-O-β-d-glucopyranoside**. MD simulations were carried out to determine the stability of the interactions of ligand-protein docked complexes. In MD simulations, the stability of the protein (6LU7) with mechanism-based inhibitor (N3)

Journal of Chemical Health Risks
www.jchr.org
JCHR (2024) 14(4), 271-288 | ISSN:2251-6727

bound at the Targeting main protease (M ^{pro}) of SARS-CoV-2: M ^{pro} binding site was investigated using RMSD analysis of the protein backbone about the initial frame structure. The RMSD value of protein was stable between 2.3 to 3.0 Å from a 15 to 95 ns time frame it showed excellent stability with protein. The ligand RMSD was also stable between 5.4 to 6.6 Å from a 5 to 95 ns time frame (Figure 13). The RMSF plots of protein (side chains) and ligand showed few fluctuations between 0.7 to 3.0 Å respectively, and Protein residues that interact with the ligand are marked with green-colored vertical bars (Figure 14) The interactions during the 100 ns trajectory were examined, where residues Thr26, Asn142, Glu166, Asp187, Arg188, and Gln189 showed H-Bond interaction with protein, and His41 were involved in π-π stacking interactions with protein, and His41, Cys145, and Met165 were engaged in hydrophobic interactions with protein (Figure 15, 16).

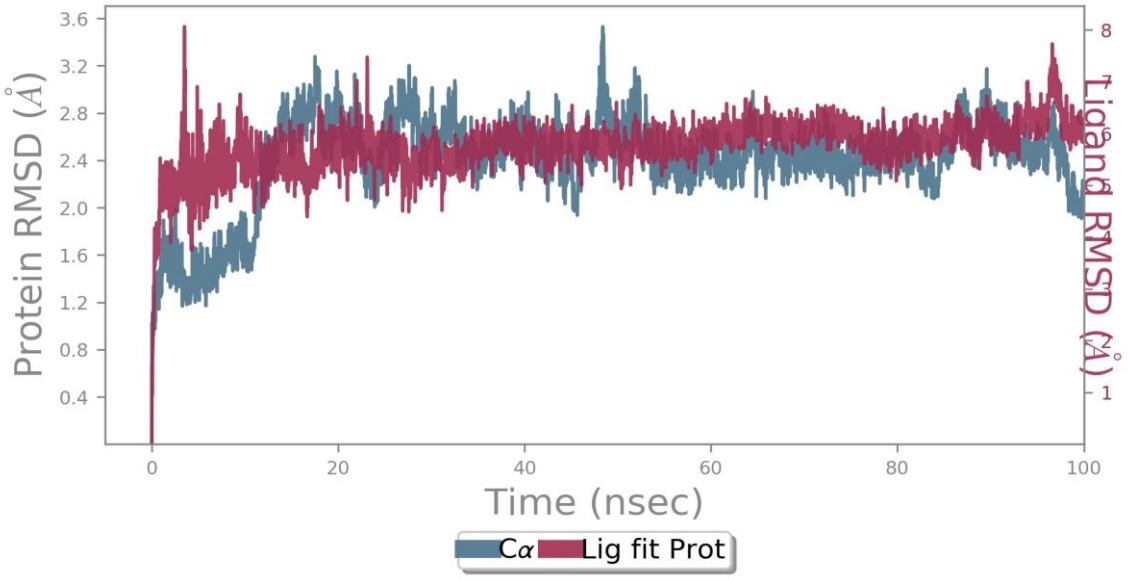

Fig.13: RMSD plot of coronavirus for COVID-19 (6LU7) with and without **isorhamnetin-3-O-β-d-glucopyranoside** as a function of time

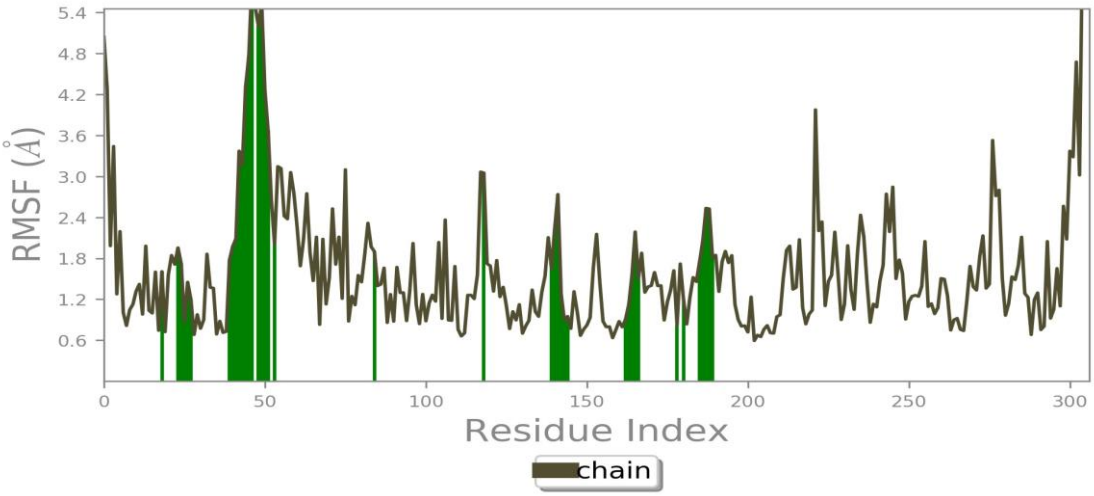

Fig.14: RMSF plot of coronavirus for COVID-19 (6LU7) with and without **isorhamnetin-3-O-β-d-glucopyranoside** at 100 ns time scale

Journal of Chemical Health Risks
www.jchr.org
JCHR (2024) 14(4), 271-288 | ISSN:2251-6727

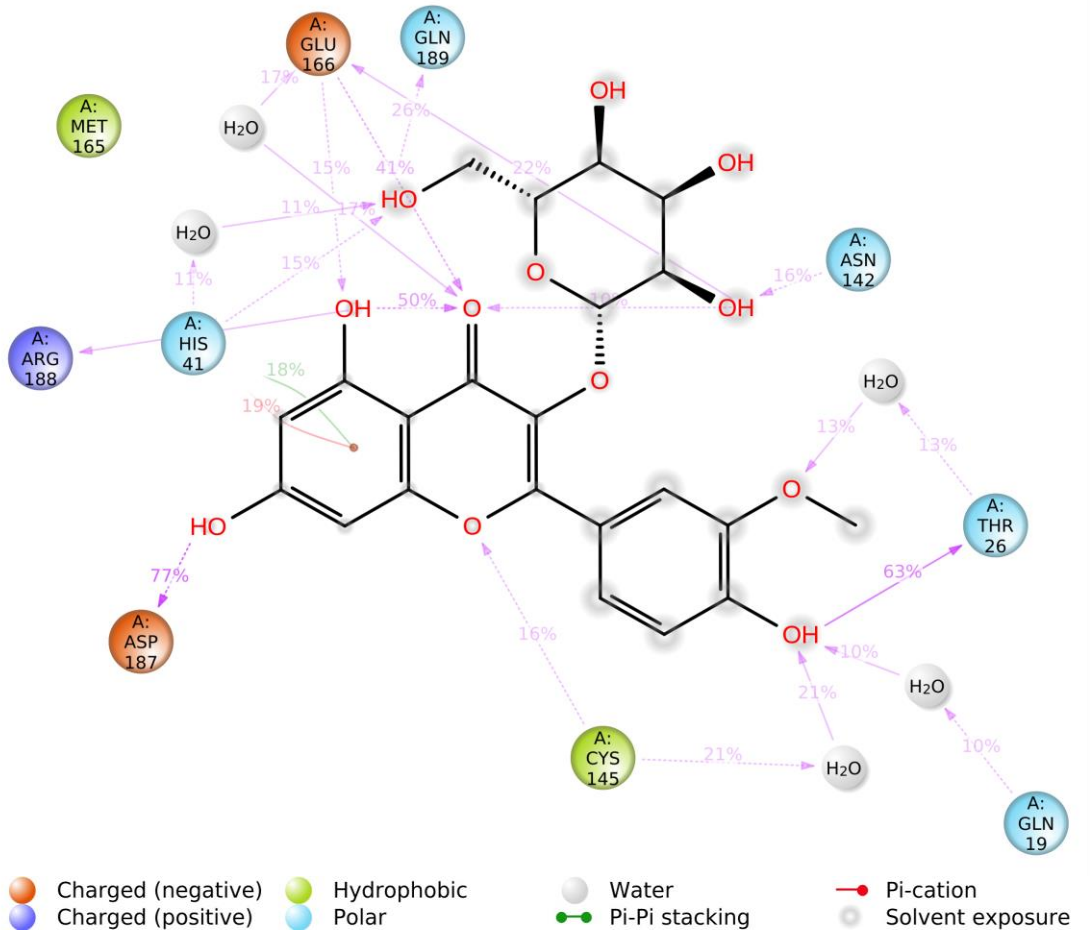

Fig.15: The interaction of top hit molecule **isorhamnetin-3-O-β-d-glucopyranoside** with coronavirus for COVID-19 (6LU7)

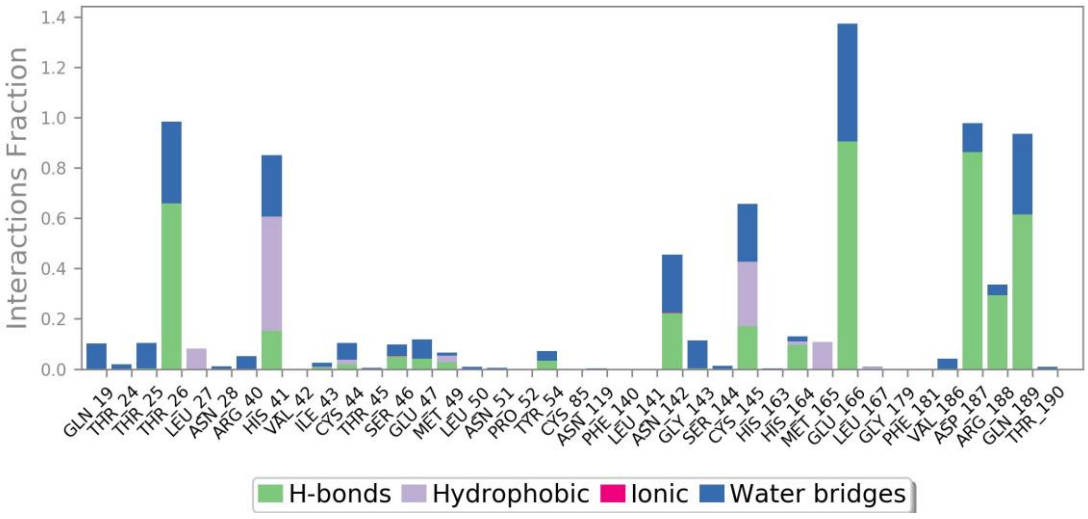

Fig.16: Protein-ligand contacts for compound **isorhamnetin-3-O-β-d-glucopyranoside**

Journal of Chemical Health Risks
www.jchr.org
JCHR (2024) 14(4), 271-288 | ISSN:2251-6727

Complex 4: 6LU7-(+) butyl-O-α-l-rhamnoside

MD simulation at 100ns was performed for top-docked compound **(+) butyl-O-α-l-rhamnoside**. MD simulations were carried out to determine the stability of the interactions of ligand-protein docked complexes. In MD simulations, the stability of the protein (6LU7) with mechanism-based inhibitor (N3) bound at the Targeting main protease (M^{pro}) of SARS-CoV-2: M^{pro} binding site was investigated using RMSD analysis of the protein backbone about the initial frame structure. The RMSD value of protein was stable between 2.0 to 2.5 Å from a 15 to 100 ns time frame with little flexibility. The ligand RMSD gets equilibration between 2.5 to 3.8 Å from a 50 to 95 ns time frame before 50 ns it showed flexibility with protein (Figure 17). The RMSF plots of protein (side chains) and ligand showed few fluctuations between 0.6 to 2.4 Å respectively, and Protein residues that interact with the ligand are marked with green-colored vertical bars (Figure 18) The interactions during the 100 ns trajectory were examined, where residues Asn142, Arg188, Gln189, and Thr190 showed H-Bond interaction with protein, and Met165, Leu167, and Pro168 were engaged in hydrophobic interactions with protein (Figure 19, 20).

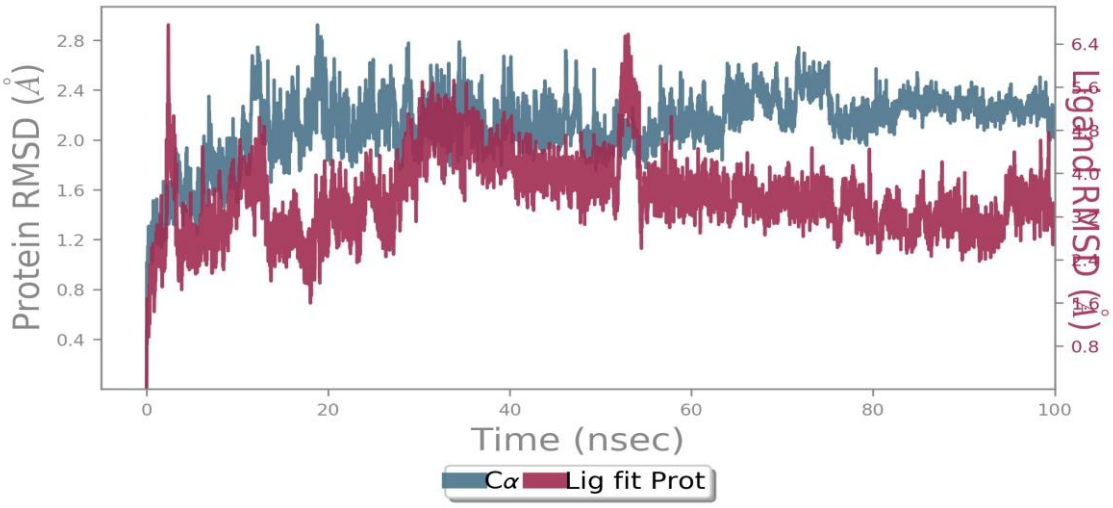

Fig.17: RMSD plot of coronavirus for COVID-19 (6LU7) with and without **(+) butyl-O-α-l-rhamnoside** as a function of time

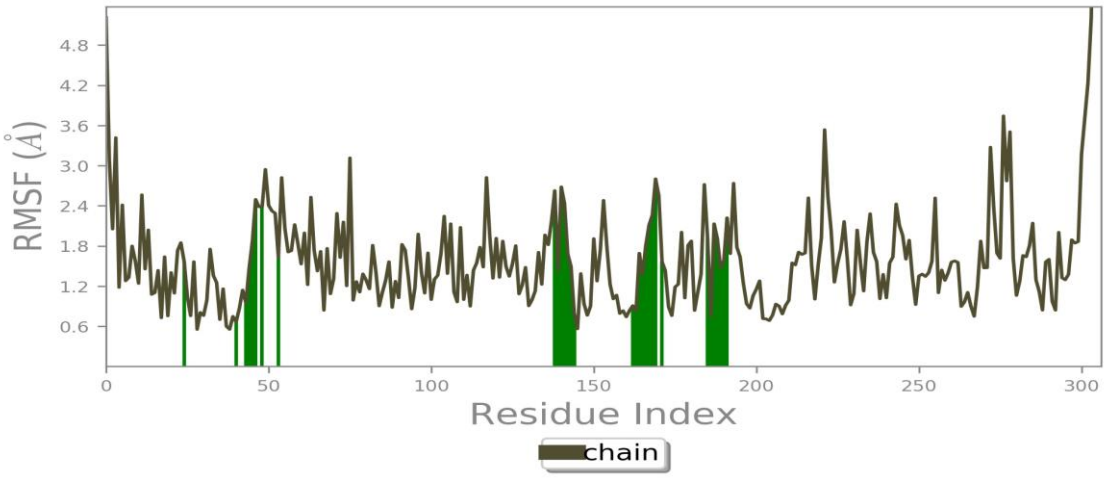

Fig.18: RMSF plot of coronavirus for COVID-19 (6LU7) with and without **(+) butyl-O-α-l-rhamnoside** at 100 ns time scale

Journal of Chemical Health Risks
www.jchr.org
JCHR (2024) 14(4), 271-288 | ISSN:2251-6727

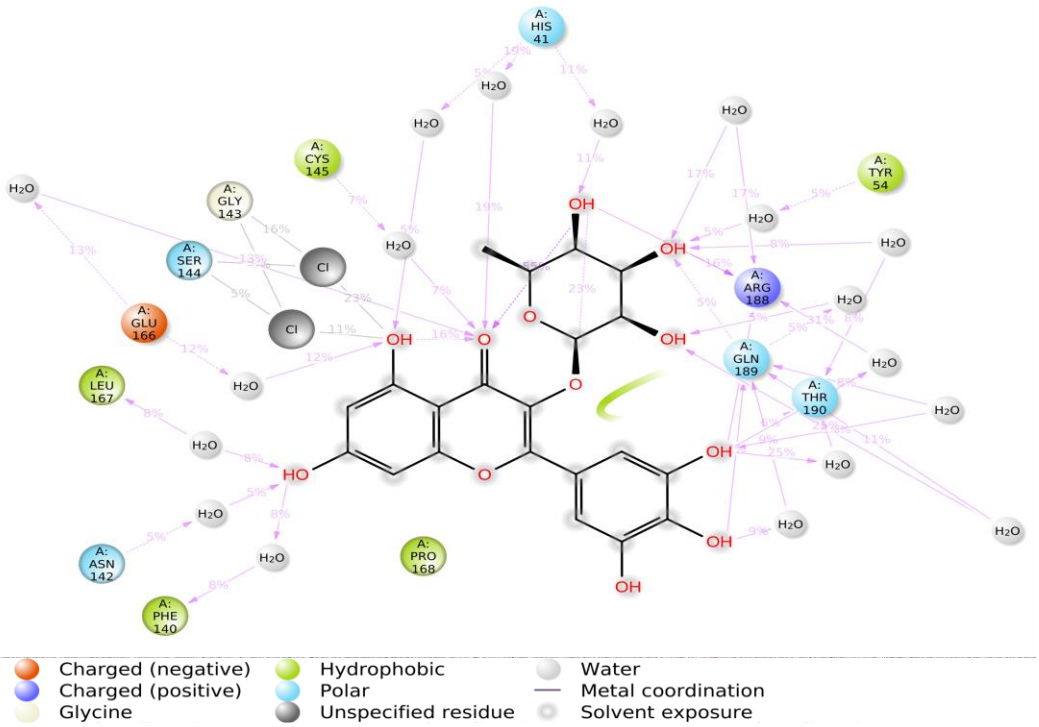

Fig.19: The interaction of top hit molecule **(+) butyl-O-α-l-rhamnoside** with coronavirus for COVID-19 (6LU7)

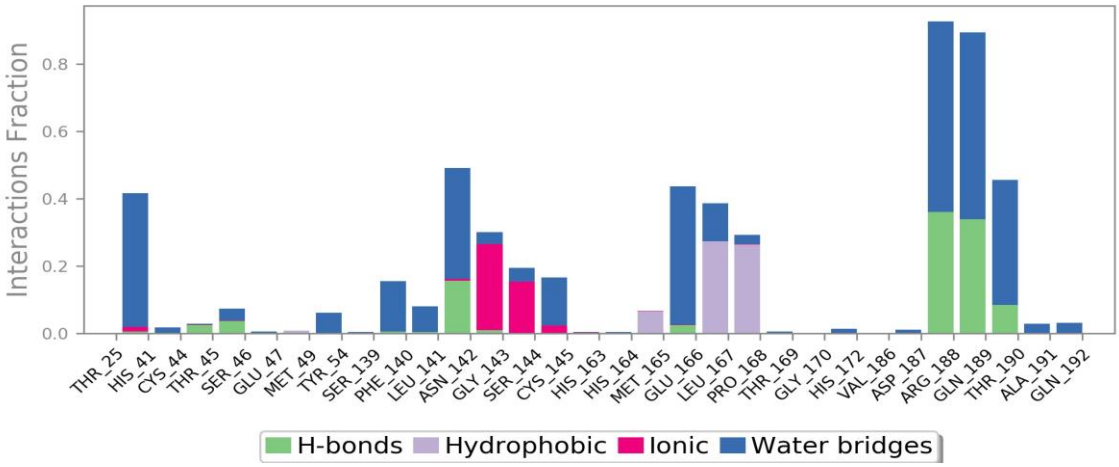

Fig.20: Protein-ligand contacts for compound **(+) butyl-O-α-l-rhamnoside**

Comparative studies

When we compare the docking and molecular dynamics studies, the top 4 compounds selected for the dynamics studies based on docking studies are the most suitable molecules according to the results. They show good binding affinity and stability during MDS simulation studies. The quercetin-3-O-β-d glucopyranoside has shown two H-bond interactions with SER144 and Thr26 during docking studies still during MDS studies it shows three H-bond interactions with Asp187, Thr26, and Gln189 with protein. The kaempferol-3-O-β-d-glucopyranoside doesn't show any H-bond interaction with protein. Still, during MDS simulation it shows H-bond interaction with Asn142, Glu166, Asp187, Arg188,

Journal of Chemical Health Risks

www.jchr.org

JCHR (2024) 14(4), 271-288 | ISSN:2251-6727

and Gln189, these results show the stability of the complex during the simulation. The isorhamnetin-3-O-β-d-glucopyranoside has shown H-bond interaction with GLU166 during docking studies, during MDS studies it shows H-bond interaction with Thr26, Asn142, Glu166, Asp187, Arg188, and Gln189. The (+) butyl-O-α-l-rhamnoside doesn't show any H-bond interaction during docking studies, during MDS simulation it shows H-bond interaction with Asn142, Arg188, Gln189, and Thr190. Comparative study shows the stability and affinity of the selected molecules toward this study.

Summary and Conclusion

COVID-19 is continuing to become a global burden on human health and economic losses remain unabated. Virtual screening remains one of the incredible approaches for the structure-based design of chemical scaffolds against a known target protein binding well within the active site. In our studies we have screened *Carissa edulis*, *Geranium Sanguin Eu*, *Guazuma Ulmifolia*, *Polygonum cuspidatum*, *Saxifraga melanocentra* containing different compounds and potential inhibitors of COVID-19. Our *in-silico* screening results indicated that the compound quercetin-3-O-β-d glucopyranoside, kaempferol-3-O-β-d-glucopyranoside, isorhamnetin-3-O-β-d-glucopyranoside, and (+) butyl-O-α-l-rhamnoside, has high potential against main protease, 3CLpro of SARS-CoV-2, and thus selected as a positive control for the design of new drug candidates based on human protease. Molecular docking analysis of quercetin-3-O-β-d glucopyranoside with **-9.2** docking score, kaempferol-3-O-β-d-glucopyranoside with **-9** docking score, isorhamnetin-3-O-β-d-glucopyranoside with **-8.9** docking score, (+) butyl-O-α-l-rhamnoside with **-8.6** docking score on the N3 inhibitor COVID-19 main protease (6LU7) protein has shown that four compounds are more efficient than the preferred compound. More potent inhibitors of N3 have been identified through docking studies. Molecular dynamics studies on these top four compounds quercetin-3-O-β-d glucopyranoside, kaempferol-3-O-β-d-glucopyranoside, isorhamnetin-3-O-β-d-glucopyranoside, and (+) butyl-O-α-l-rhamnoside revealed their binding stability and conformational changes associated with the protein-ligand complexes. RMSF for all complexes was under 3 Å. Hence, these four compounds are proposed for validation and further studies as more efficient medication for COVID-19.

References

1. Wei, M., Yang, N., Wang, F., Zhao, G., Gao, H. and Li, Y., 2020. Epidemiology of coronavirus disease 2019 (COVID-19) caused by severe acute respiratory syndrome coronavirus 2 (SARS-CoV-2). Disaster medicine and public health preparedness, 14(6), pp.796-804.
2. Sharma, A., Tiwari, S., Deb, M.K. and Marty, J.L., 2020. Severe acute respiratory syndrome coronavirus-2 (SARS-CoV-2): a global pandemic and treatment strategies. International journal of antimicrobial agents, 56(2), p.106054.
3. Bchetnia, M., Girard, C., Duchaine, C. and Laprise, C., 2020. The outbreak of the novel severe acute respiratory syndrome coronavirus 2 (SARS-CoV-2): A review of the current global status. Journal of infection and public health, 13(11), pp.1601-1610.
4. Al-Qahtani, A.A., 2020. Severe acute respiratory syndrome coronavirus 2 (SARS-CoV-2): emergence, history, basic and clinical aspects. Saudi journal of biological sciences, 27(10), pp.2531-2538.
5. Madabhavi, I., Sarkar, M. and Kadakol, N., 2020. COVID-19: a review. Monaldi Archives for Chest Disease, 90(2).
6. Neamah, S.R., 2020. Comparison between symptoms of COVID-19 and other respiratory diseases. Electronic Journal of Medical and Educational Technologies, 13(3), p.em2014.
7. Çalıca Utku, A., Budak, G., Karabay, O., Güçlü, E., Okan, H.D. and Vatan, A., 2020. Main symptoms in patients presenting in the COVID-19 period. Scottish medical journal, 65(4), pp.127-132.
8. Hane, F.T., Robinson, M., Lee, B.Y., Bai, O., Leonenko, Z. and Albert, M.S., 2017. Recent progress in Alzheimer's disease research, part 3: diagnosis and treatment. Journal of Alzheimer's disease, 57(3), pp.645-665.
9. Tse, L.V., Meganck, R.M., Graham, R.L. and Baric, R.S., 2020. The current and future state of vaccines, antivirals and gene therapies against emerging coronaviruses. Frontiers in microbiology, 11, p.658.
10. Oprea, T.I., Bologa, C.G., Brunak, S., Campbell, A., Gan, G.N., Gaulton, A., Gomez, S.M., Guha, R., Hersey, A., Holmes, J. and Jadhav, A., 2018. Unexplored therapeutic opportunities in the human genome. Nature reviews Drug discovery, 17(5), pp.317-332.

Journal of Chemical Health Risks

www.jchr.org

JCHR (2024) 14(4), 271-288 | ISSN:2251-6727

11. Sugiki, T., Kobayashi, N. and Fujiwara, T., 2017. Modern technologies of solution nuclear magnetic resonance spectroscopy for three-dimensional structure determination of proteins open avenues for life scientists. Computational and structural biotechnology journal, 15, pp.328-339.
12. Pinzi, L. and Rastelli, G., 2019. Molecular docking: shifting paradigms in drug discovery. International journal of molecular sciences, 20(18), p.4331.
13. Satoskar, R.S. and Bhandarkar, S.D., 2020. Pharmacology and pharmacotherapeutics. Elsevier India.
14. Attah, A.F., Fagbemi, A.A., Olubiyi, O., Dada-Adegbola, H., Oluwadotun, A., Elujoba, A. and Babalola, C.P., 2021. Therapeutic potentials of antiviral plants used in traditional african medicine with COVID-19 in focus: a Nigerian perspective. Frontiers in pharmacology, 12, p.596855.
15. Abookleesh, F.L., Al-Anzi, B.S. and Ullah, A., 2022. Potential antiviral action of alkaloids. Molecules, 27(3), p.903.
16. Musarra-Pizzo, M., Pennisi, R., Ben-Amor, I., Mandalari, G. and Sciortino, M.T., 2021. Antiviral activity exerted by natural products against human viruses. Viruses, 13(5), p.828.
17. Arip, M., Selvaraja, M., Tan, L.F., Leong, M.Y., Tan, P.L., Yap, V.L., Chinnapan, S., Tat, N.C., Abdullah, M., K, D. and Jubair, N., 2022. Review on plant-based management in combating antimicrobial resistance-mechanistic perspective. Frontiers in Pharmacology, 13, p.879495.
18. Jha, V., Macchia, M., Tuccinardi, T. and Poli, G., 2020. Three-dimensional interactions analysis of the anticancer target c-src kinase with its inhibitors. Cancers, 12(8), p.2327.
19. Benhander, G.M. and Abdusalam, A.A.A., 2022. Identification of potential inhibitors of SARS-CoV-2 main protease from Allium roseum L. molecular docking study. Chemistry Africa, 5(1), pp.57-67.
20. Tachoua, W., Kabrine, M., Mushtaq, M. and Ul-Haq, Z., 2020. An in-silico evaluation of COVID-19 main protease with clinically approved drugs. Journal of molecular graphics and modelling, 101, p.107758.
21. Durdagi, S., Aksoydan, B., Dogan, B., Sahin, K. and Shahraki, A., 2020. Screening of clinically approved and investigation drugs as potential inhibitors of COVID-19 main protease: a virtual drug repurposing study.
22. Arjomand, M.R., Habibi-Rezaei, M., Ahmadian, G., Hassanzadeh, M., Karkhane, A.A., Asadifar, M. and Amanlou, M., 2016. Deletion of loop fragment adjacent to active site diminishes the stability and activity of exo-inulinase. International journal of biological macromolecules, 92, pp.1234-1241.
23. Das, B., 2015. Qsar analysis, docking & molecular dynamics simulation of several antimicrobial compounds and receptors (Doctoral dissertation, University of North Bengal).
24. Salo, H., 2016. Computational approach towards sirtuin inhibitors: application of molecular docking methods (Doctoral dissertation, Itä-Suomen yliopisto).
25. Pissurlenkar, R.R., Shaikh, M.S., Iyer, R.P. and Coutinho, E.C., 2009. Molecular mechanics force fields and their applications in drug design. Anti-Infective Agents in Medicinal Chemistry (Formerly Current Medicinal Chemistry-Anti-Infective Agents), 8(2), pp.128-150.
26. Talluri, S., 2021. Molecular docking and virtual screening based prediction of drugs for COVID-19. Combinatorial Chemistry & High Throughput Screening, 24(5), pp.716-728.
27. Apostolakis, J., Plückthun, A. and Caflisch, A., 1998. Docking small ligands in flexible binding sites. Journal of Computational Chemistry, 19(1), pp.21-37.
28. Josaphat, F. and Fadlan, A., 2023. Molecular Docking of Acetylacetone-Based Oxindole Against Indoleamine 2, 3-Dioxygenase: Study of Energy Minimization. Walisongo Journal of Chemistry, 6(2), pp.149-157.
29. Guilbert, C. and James, T.L., 2008. Docking to RNA via root-mean-square-deviation-driven energy minimization with flexible ligands and flexible targets. Journal of chemical information and modeling, 48(6), pp.1257-1268.
30. Rana, K.M., Maowa, J., Alam, A., Dey, S., Hosen, A., Hasan, I., Fujii, Y., Ozeki, Y. and Kawsar, S.M., 2021. In silico DFT study, molecular docking, and ADMET predictions of cytidine analogs with antimicrobial and anticancer properties. In Silico Pharmacology, 9, pp.1-24.

31. Ortiz, A.R., Pisabarro, M.T., Gago, F. and Wade, R.C., 1995. Prediction of drug binding affinities by comparative binding energy analysis. Journal of medicinal chemistry, 38(14), pp.2681-2691.
32. Li, X., Zhang, W., Qiao, X. and Xu, X., 2007. Prediction of binding for a kind of non-peptic HCV NS3 serine protease inhibitors from plants by molecular docking and MM-PBSA method. Bioorganic & Medicinal Chemistry, 15(1), pp.220-226.
33. Di, L. and Kerns, E.H., 2015. Drug-like properties: concepts, structure design and methods from ADME to toxicity optimization. Academic press.
34. Singh, M.B., Sharma, R., Kumar, D., Khanna, P., Khanna, L., Kumar, V., Kumari, K., Gupta, A., Chaudhary, P., Kaushik, N. and Choi, E.H., 2022. An understanding of coronavirus and exploring the molecular dynamics simulations to find promising candidates against the Mpro of nCoV to combat the COVID-19: A systematic review. Journal of infection and public health, 15(11), pp.1326-1349.
35. Yadav, P., Rana, M. and Chowdhury, P., 2021. DFT and MD simulation investigation of favipiravir as an emerging antiviral option against viral protease (3CLpro) of SARS-CoV-2. Journal of Molecular Structure, 1246, p.131253.
36. Berkane, A., Kundu, N., Munia, A.A., Chakrabarty, B., Utpal, B.K., Kumar, N., Vijay, D., Bourhia, M., Jardan, Y.A.B., Abdelkrim, G. and da Silva, M.K., 2024. Development of new drug candidate for the inhibition of Nipah virus phosphoprotein by Quercetin Derivatives through in silico drug design approaches. Journal of the Indian Chemical Society, p.101196.